ORIGINAL ARTICLE

Ischaemia–reperfusion injury in orthotopic mouse lung transplants – a scanning electron microscopy study

Alice Draenert*, Klaus Marquardt†, Ilhan Inci*, Alex Soltermann‡, Walter Weder* and Wolfgang Jungraithmayr*

Division of Thoracic Surgery, University Hospital Zurich, Zurich, Switzerland, †Department of Image Analysis and Microscopy, University Hospital Zurich, Zurich, Switzerland and ‡Institute for Surgical Pathology, University Hospital Zurich, Zurich, Switzerland

Summary

Lung ischaemia-reperfusion (I/R) injury remains a major cause of graft failure in lung transplantation (Tx). With the implementation of orthotopic lung Tx in mice, a physiological model on the base of a perfused and ventilated graft became available for the investigation of I/R injury. Using the scanning electron microscopy (SEM) technique, we here present an analysis of early and late morphological changes of pulmonary I/R injury. Syngeneic lungs were orthotopically transplanted between C57BL/6 mice. Grafts were exposed to 2 h of cold ischaemia. Transplants and right lungs were examined by SEM with corresponding haematoxylin–eosin histology 30 min and 4 h after reperfusion. Thirty minutes after reperfusion, the alveolar surface of transplants showed a discontinued lining of surfactant, while the lining of the non-transplanted lung was normal. Within the graft, leucocytes displayed an irregular surface with development of pseudopodia, and microvilli were detected on the membrane of pneumocytes. At 4 h after reperfusion, leucocytes significantly increased in numbers within the alveolar space. Also, the number of microvilli on pneumocytes increased significantly. Similar to these, the endothelium of vessels increasingly developed microvilli from 30 min towards 4 h after reperfusion. The airways of transplanted grafts showed mild changes with thickening of the bronchial epithelium and a destruction of kinocilia. Taken together, SEM detects pathological events of I/R that are previously not described in normal histology. These findings may influence the interpretation of studies investigating the I/R injury in the mouse model of lung Tx.

Keywords

Ischaemia-reperfusion injury, orthotopic mouse lung transplantation, scanning electron microscopy

Ischaemia-reperfusion (I/R) injury is a major cause for early graft dysfunction after lung transplantation (Tx) (Lee & Christie 2009). Cells of the innate immune system but also lung parenchymal cells contribute to graft injury by the generation of reactive oxygen species (Ovechkin *et al.* 2007) eventually leading to structural damage of the graft with development of interstitial and intra-alveolar oedema, and loss of integrity of the blood air barrier.

The mouse model of orthotopic lung Tx has been recently introduced as a valuable tool to study immunological and non-immunological events after lung Tx (Okazaki *et al.* 2007; Jungraithmayr *et al.* 2009). While pathomorphological changes of I/R injury were previously described on the basis of the hilar clamping technique (Zanotti *et al.* 2009), the model of orthotopic Tx provides a physiological basis to study I/R injury.

The technique of scanning electron microscopy (SEM) allows for the analysis of the three-dimensional structure of the lung disclosing morphological changes and interactions between cells and the pulmonary tissue (Hsia *et al.* 2010). SEM has been shown to detect pathological changes in a rabbit *ex vivo* model of I/R (Premaratne *et al.* 2000) and proved to be an important method to quantify ultrastructural changes of I/R injury (Hasaniya *et al.* 2009).

As the model of orthotopic lung Tx in mice is increasingly applied in experimental studies, we here provide a thorough SEM analysis of the early and late phenomena of I/R injury in mouse lung transplants, and the non-transplanted right lung.

Material and methods

Animals and experimental setting

Specific pathogen-free inbred male mice (Fuellinsdorf, Zurich, Switzerland), weighing 25–30 g, 10–14 weeks old, were used. Animals received adequate care according to *The Principles of Laboratory Animal Care* (National Institutes of Health, promulgated in 1985, most recently revised in 1996). Orthotopic, syngeneic lung Tx between C57BL/6 mice (H-2K^b) ($n = 2$) was performed as described before (Jungraithmayr *et al.* 2009). The cold ischaemic time was 2 h. The transplanted graft and the right, non-transplanted lung were analysed at two time points, at 30 min and 4 h after reperfusion.

Lung recovery

Animals were intubated, anaesthetized, and a laparosternotomy was performed as described (Jungraithmayr *et al.* 2009). Ventilation was maintained applying a tidal volume of 1 ml with a positive end-expiratory pressure of 2 mbar, which remained unchanged until removal of the heart and lungs. The lungs were first flushed with 10–15 ml of 0.9% normal saline solution at a pressure of 10 cm H_2O via the pulmonary artery, followed by the perfusion of 10 ml of a 2% glutaraldehyde-containing phosphate buffer solution according to Bachofen *et al.* (Bachofen *et al.* 1982; Fehrenbach *et al.* 1999). The ventilation was stopped during glutaraldehyde fixation. The inflow of the fixation medium lasted 2 min. The removal of the heart and lung was performed *en bloc* with inflated lungs at two-third. The fixation procedure was maintained for 24 h by immersion in an equivalent 2% glutaraldehyde-containing phosphate buffer solution as described earlier and stored at 4 °C.

Light microscopy and histology

Specimen preparation was accomplished by using a photo documentation system (Leica Z16 APO, Heerbrugg, Switzerland). After removal of heart and lungs, the whole lung was cut into half in the frontal plane, both the transplanted and the right, non-transplanted lung. Sections were taken from peripheral and central parts of each to ensure objective and accurate sampling with equal probability of the samples. These sections were used for SEM and Haematoxylin and Eosin (H&E) staining.

Immunohistochemistry for ICAM-1

Immunohistochemistry for ICAM-1 (CD54) was performed according to previously established protocols using micro-

wave treatment as an antigen retrieval method (Graf *et al.* 2002). The primary antibody for ICAM-1 (AbD Serotec; Morphosys, Oxford, UK) was applied in a dilution of 1:1500. Linked to a biotinylated secondary antibody (Vector Laboratories, Burlingame, CA, USA), the signal was detected with 3, 3′-diaminobenzidine tetrahydrochloride (DAB), which produces a brown colour at the site of the reaction. Sections were lightly counterstained with Mayer's haematoxylin.

Scanning electron microscopy

The transplanted and the right, non-transplanted lungs were prepared for SEM as described. Sections were then dehydrated in ethanol, using increasing ethanol concentrations from 10% to 100%, with four final washing steps in 100% ethanol. Each washing step required 20–30 min. Next, critical-point drying (BAL-TEC CPD 030; Balzal, Lichtenstein) and washing with 11 cycles in liquid carbon dioxide. After sputtering with platinum in an argon chamber (BAL-TEC, SDC 500 EVN; Balzal Lichtenstein), the scanning procedure was started, and images were recorded (Zeiss Supra 50 VP; Zeiss, Oberkochen, Germany).

Statistics

Data analysis was performed using SPSS for Windows 15.0 (SPSS, Inc., Chicago, IL, USA). Unbiased sampling was ensured using the modified systematic uniform random sampling method (Hsia *et al.* 2010). A lattice grid was laid over the sections, and every fifth grid square measuring 40×40 μm (equivalent to a number of 18 alveoli) was selected. On top of this, a new grid was laid, every tenth square measuring 2×2 μm was selected, and leucocytes and microvilli (MV) were counted. The numbers of leucocytes and MV were expressed as mean ± Standard Error of Mean (SEM). For categorical values, Pearson's chi-square test was used. The Mann–Whitney *U*-test was performed to compare the differences between the two groups. A *P* value < 0.05 was considered to be statistically significant.

Results

Alveolar space

The right, non-transplanted lung showed a normal alveolar histoarchitecture with only few immune cells that were attached to a smooth alveolar surface (Figure 1a,b). Thirty minutes after reperfusion, the alveolar wall was thickened because of oedema (Figure 1c). The surface of the alveolar wall (pneumocytes type I) was covered by MV and appeared roughened by the development of these MV (Figure 1e). Furthermore, few MV were already present on pneumocytes type II (Figure 1d). Activated macrophages (M) were identified by the development of pseudopodia (Pp) (Figure 1e). A thin layer, suggestive to be the surfactant lining, covered the alveolar wall in a discontinuous manner. Lymphocytes were few in numbers.
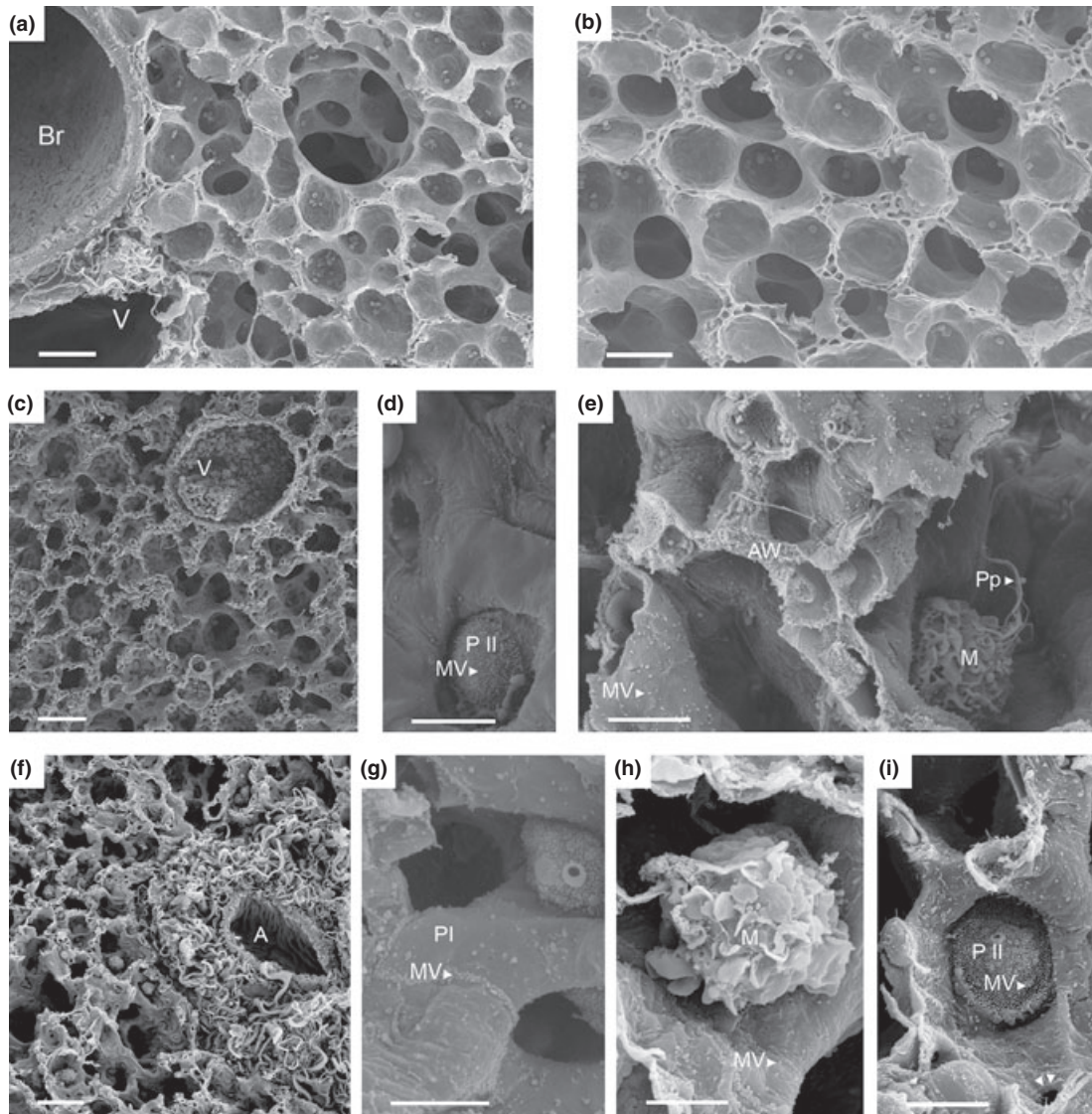
Figure 1 Alveolar tissue from right, non-transplanted lung, and transplanted lung, 30 min and 4 h after reperfusion. (a, b) Normal alveolar tissue of the non-transplanted, right lung; (c–e) transplanted graft 30 min after reperfusion, with oedema formation of the alveolar wall, and the development of microvilli (MV) on the surface of pneumocytes type II (P II) (d, e, arrow), macrophages (M) display pseudopodia (Pp) (e, arrow); (f–i) transplanted graft 4 h after reperfusion with perivascular widening (f), increased numbers of MV (g, h, i, arrow), that are predominantly located on the margin between pneumocytes type I (g, arrow), and enlarged alveolar M (h). Kohn's pore becomes visible (i, double arrow). Br, bronchus; AW, alveolar wall; V, vein; A, artery; M, macrophage; MV, micro-villi; P I/II, pneumocytes type I/II Pp, pseudopodia; Tx, transplantation. (a–c, f) Scale bare = 40 μm. (d, e, g–i) Scale bar = 5 μm.

Four hours after reperfusion, the thickening of the alveolar wall increased (Figure 1f), MV now developed predominantly along the border between pneumocytes type I (Figure 1g). Also, MV significantly increased in numbers and became longer on pneumocytes type II (Figures 1g,i, and 2). In contrast, pneumocytes types II demarcate, and the surface separated increasingly from each other when compared to pneumocytes type I (Figure 1i). Pneumocytes type II showed extensive exocytosis and an enlargement of cell size (Figure 1i). Leucocyte numbers increased significantly (Figure 3); they enlarged in size and displayed a roughened surface (Figure 1h). Perforations of 1 μm in diameter developed within the alveolar wall (Kohn's pore) (Figure 1i). These perforations are equivalent to Kohn's pores that are not visible under normal conditions, because of the covering by a continuous lining of surfactant (Bastacky & Goerke 1992). In contrast, no Kohn pores were detectable in the right, non-transplanted lung that was subjected to the same treatment as the transplanted lung.

Airways

The right, non-transplanted lung showed a normal histo-architecture without impairment of the kinocilia. There was regular mucus production overall (Figure 4a,b).
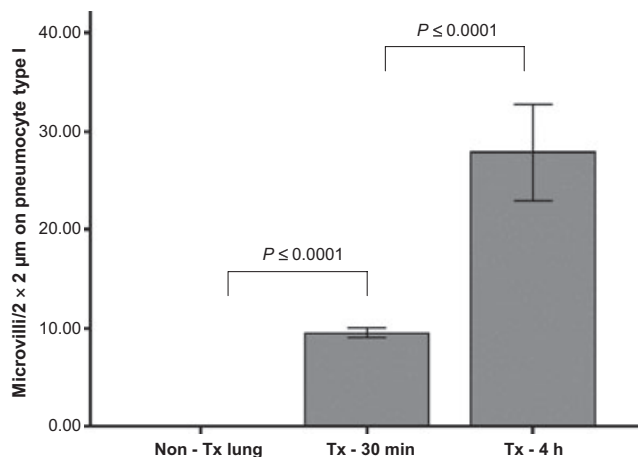
Figure 2 Number of microvilli (MV) per 2×2 μm on pneumocytes type I at different time points: non-Tx lung calculated as time zero, Tx-30 min, Tx-4 h after reperfusion. Tx lungs 4 h after reperfusion show significant higher numbers of MV compared to Tx lungs 30 min after reperfusion (27.9 ± 4.9 vs. 9.5 ± 0.5; $P \leq 0.0001$), and Tx lung 30 min after reperfusion showed significantly more numbers of MV compared to non-transplanted lung (9.5 ± 0.5 vs. 0.0 ± 0.0; $P \leq 0.0001$). Non-Tx Lung, non-transplanted lung; Tx-30 min, transplanted lung, 30 min after reperfusion; Tx-4 h, transplanted lung, 4 h after reperfusion.
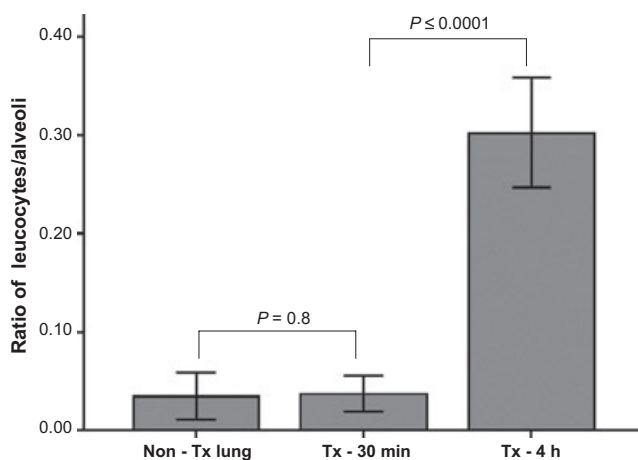

Figure 3 Ratio of leucocytes per alveoli on different time points: non-Tx lung calculated as time zero, Tx-30 min, Tx-4 h after reperfusion. Tx lungs 4 h after reperfusion show significant influx of leucocytes compared to Tx lungs 30 min after reperfusion (0.30 ± 0.06 vs. 0.04 ± 0.02; $P \leq 0.0001$). Numbers of leucocytes from Tx lung 30 min after reperfusion did not differ from non-transplanted lung (0.04 ± 0.02 vs. 0.03 ± 0.02; $P = 0.8$). Non-Tx lung, non-transplanted lung; Tx-30 min, transplanted lung 30 min after reperfusion; Tx-4 h, transplanted lung 4 h after reperfusion.

Thirty minutes after reperfusion, the bronchial wall was mildly thickened because of the development of oedema (Figure 4c,d). Clara cells showed slight changes on the surface with a rounding and clumping of the microvilli (Figure 4e), yet, moderate amounts of mucus were released

upon exocytosis. The surface of the epithelium was partially covered by water because of oedema formation (Figure 4f).

Four hours after reperfusion, Clara cells showed increased exocytosis. Kinocilia on the epithelium appeared to be slightly reduced (Figure 4g,h). No immune cells or leucocytes were found on the surface of airways at that time.

Pulmonary vessels

The right, non-transplanted lung showed a smooth endothelium of veins and arteries (Figure 5a,b). The perivascular tissue was unchanged, there were no adhesions nor were there invasion of leucocytes.

Thirty minutes after reperfusion, the transplanted graft showed multiple thrombi within the vessels (Figure 5c). However, in patent vessels (Figure 5d), the endothelium showed the development of MV, and few passenger cells were adhesive to the endothelium (Figure 5e). The subendothelial, perivascular space of arteries was widened.

Four hours after reperfusion, the widening of the perivascular space of arteries increased severely, and this was accompanied by a loss of the histological fibre network of the perivascular space (Figure 1f). A mild intra-alveolar oedema developed (Figure 5c), and the endothelium of the vascular wall was corrugated (Figure 5f). Moreover, the surface of the endothelium was covered by MV (Figure 5g). Activated leucocytes, although less than those in the alveolar space, adhered to the endothelium (Figure 5g). Leucocytes adherent to the endothelium were smaller in diameter compared to M within the alveolar space.

Histology

H&E staining of corresponding SEM samples revealed a normal histoarchitecture from non-transplanted lungs (Figure 6a,b). Thirty minutes after reperfusion, few mononuclear cells infiltrated into the graft with a moderate thickening of the alveolar wall (Figure 6c,d). In contrast, 4 h after reperfusion, leucocytes and macrophages accumulated increasingly in the alveolar space but also into the alveolar wall. Furthermore, a perivascular oedema together with a mild intra-alveolar oedema developed with a pronounced thickening of the alveolar wall (Figure 6e,f).

ICAM-1 expression after ischaemia-reperfusion

Non-transplanted lungs showed a fine lining of ICAM-1 (CD54) staining on the endothelium (Figure 7a). In contrast, staining for ICAM-1 was enhanced on the endothelium in transplanted grafts at 30 min of reperfusion (Figure 7b), which increased strongly in transplanted lungs at 4 h of reperfusion (Figure 7c).

Discussion

In this study, pathomorphological changes of ischaemia-reperfusion injury in mouse lung transplants were analysed by
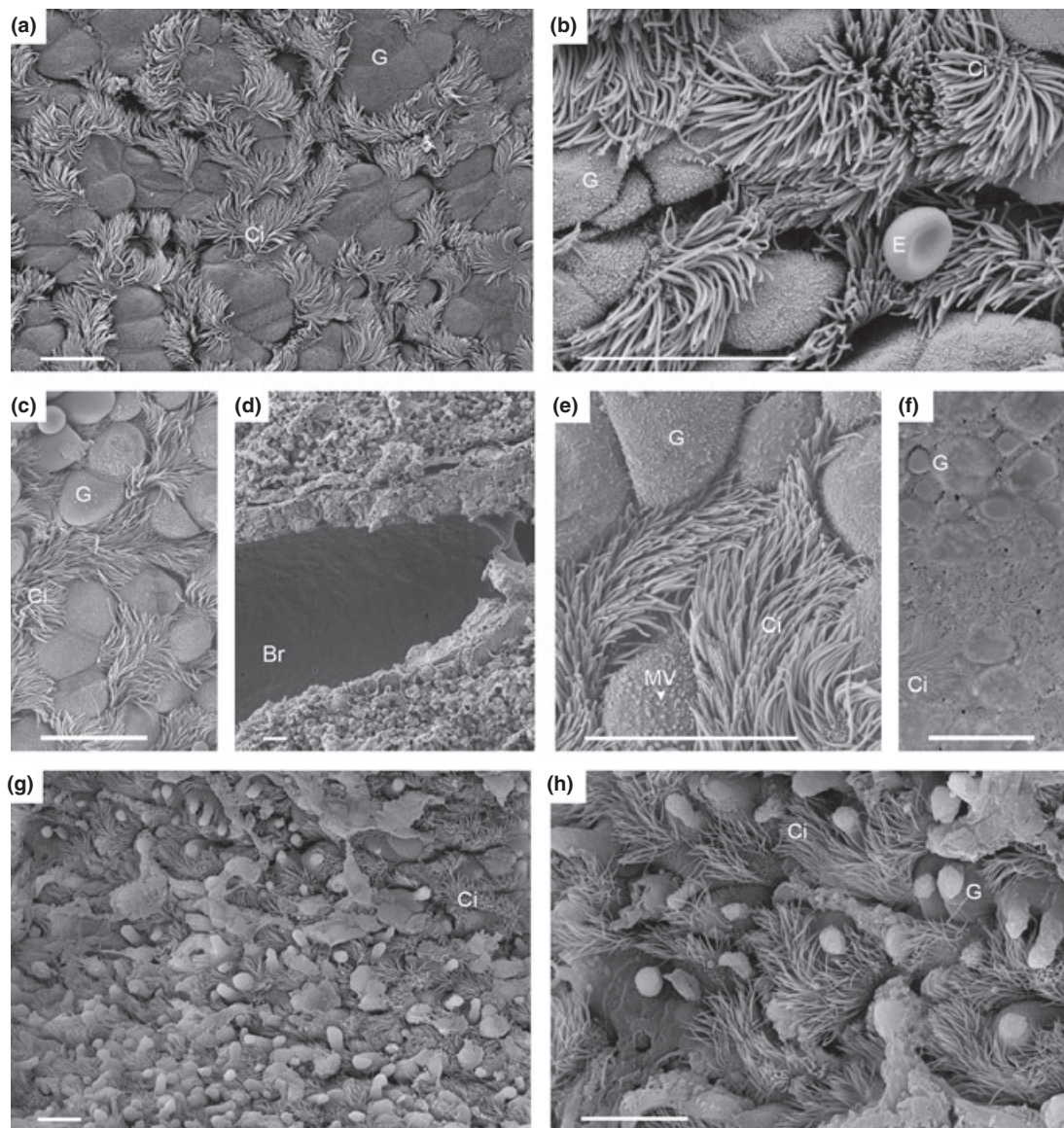
Figure 4 Respiratory tract from right, non-transplanted lung, and transplanted lung, 30 min and 4 h after reperfusion. (a, b) right, non-transplanted lung, normal bronchial tissue with goblet cells and cilia-cells, an erythrocyte (E) as a reference cell lying over bronchial tissue (b); (c–f) transplanted graft 30 min after reperfusion; Microvilli (MV) at the surface of goblet cells have a rounder form and are shorter and clumped (e, arrow) compared to MV depicted in b. The epithelium is partially covered with fluid collection because of oedema (f). (g, h) transplanted graft 4 h after reperfusion shows bronchioles with increased exocytosis of goblet cells, and a decline in numbers of cilia-cells. Br, bronchus; G, goblet cell; Ci, ciliated cell; E, erythrocyte. (a–h) Scale bar = 10 μm.

scanning electron microscopy at two different time points of reperfusion. As an early event, we found a discontinuity of the alveolar surface lining 30 min after reperfusion, suggestive to be a lack of surfactant on the surface of the alveolar space. Leucocytes were already present 30 min after reperfusion and increased in numbers at 4 h. These cells showed a roughened surface considered to be in an activated state. Furthermore, pneumocytes developed microvilli at 30 min after reperfusion that increased significantly in numbers at 4 h. This phenomenon could also be observed on the endothelium of vessels, while airways of the transplanted graft changed moderately.

Experimental animal studies defined the injury from reperfusion to develop in a biphasic manner (Eppinger *et al.* 1995). The late phase seems to be dependent on neutrophil sequestration (Eppinger *et al.* 1997), while the early phase is neutrophil independent and usually occurs within 30 min of reperfusion. In line with this observation, we found activated leucocytes in the alveolar space at the early time point and in increasing numbers at 4 h of reperfusion. These cells could be nicely identified in the stage of arrest, adherence, but also transmigrating on the endothelium of vessels, a process that requires the presence of ICAM-1, found on the
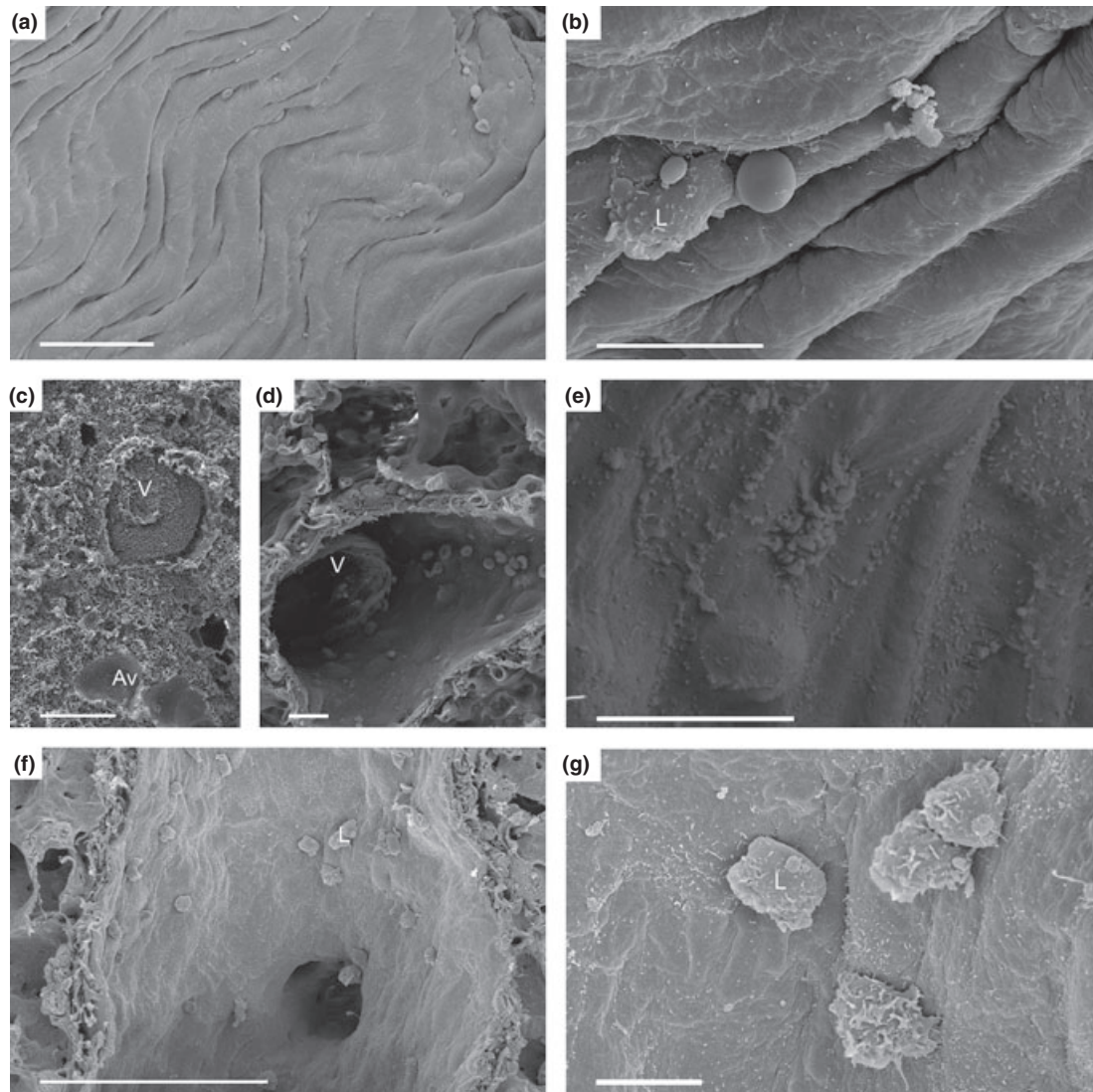
Figure 5 Endothelium from vessels from right, non-transplanted lung, and transplanted lung, 30 min and 4 h after reperfusion. (a, b) right, non-transplanted lung with regular endothelial lining with few leucocytes adherent to the endothelium. (c–e) transplanted graft 30 min after reperfusion with moderate endothelial changes with development of few microvilli (MV) (e), adhesion of few cells, but with formation of multiple thrombi. (f, g) transplanted graft, 4 h after reperfusion, with increased formation of MV (g) and adhesion of numerous leucocytes. Av, alveoli; L, leucocyte; V, vein. (a, c, f) Scale bar = 100 μm. (b, d, e, g) Scale bar = 10 μm.

endothelium of vessels in increasing amounts on I/R-injured specimens. Surprisingly, leucocytes were found in smaller numbers within the vessel compared to the alveolar space. We speculate that this is because of the washing out effect by the solution with which the lung was perfused prior to the application of glutaraldehyde. Another explanation for the higher amount of leucocytes within the alveolar space could be that mononuclear cells transmigrate very early through the endothelium into the perivascular and alveolar space. Although the endothelium is thought to play a central role in initiating I/R injury, we found only mild signs of inflammation on the endothelium at both time points.

Before the influx of neutrophils occurs, M play an important role as a first cell line defence already minutes after rep-

erfusion. As those M are present early after reperfusion injury, they seem to be resident M that become activated. The activation status in SEM could be identified by the development of Pp. Pp are generally recognized as a sign of M activation beside that they release pro-inflammatory cytokines. Although morphologically distinct from Pp, we observed also extensions on pneumocytes that have been described in electron microscopy studies before. In these, they were defined as microvilli (Dobbs *et al.* 2010). They develop as cellular membrane protrusions that increase the surface area of cells and are involved in the absorption, secretion, cellular adhesion, and mechanotransduction upon stress or injury to the cells. In response to I/R, we interpret the development of MV occurring already 30 min after
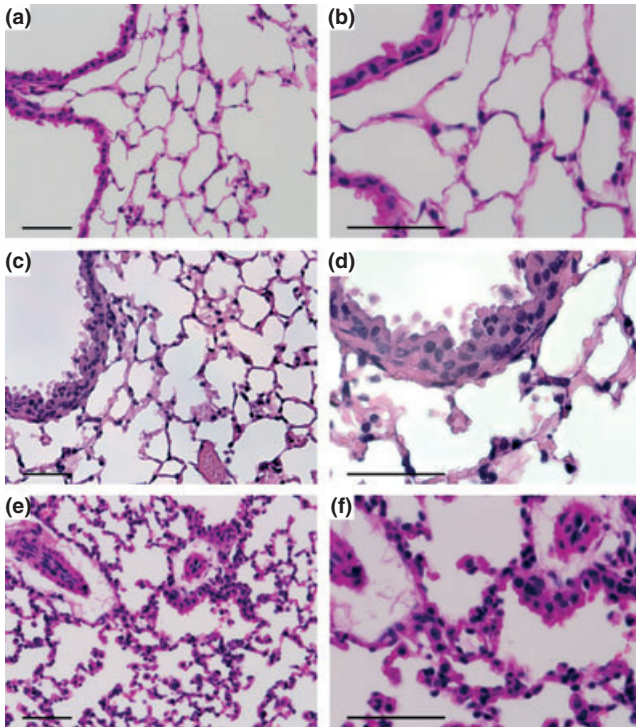
Figure 6 Histology, haematoxylin and eosin (H&E) of corresponding samples from SEM: (a, b) right, non-transplanted lung with normal histoarchitecture. (c, d) Thirty minutes after reperfusion with few infiltrates of mononuclear cells and moderate thickening of the alveolar wall. (e, f) Four hours after reperfusion with increased accumulation of leucocytes and macrophages, paralleled by perivascular oedema and more severe thickening of the alveolar wall. (a–f) Scale bar = 50 μm.

Figure 7 Immunohistochemical staining of ICAM-1. Non-transplanted lungs show a fine lining of ICAM-expression on the endothelium of the vessel. In contrast, transplanted lungs that were exposed to 2 h of ischaemia and 30 min of reperfusion, the endothelium increasingly stains positive for ICAM-1 (b) while transplanted grafts at 4 h of reperfusion revealed a strong staining for ICAM-1 (c). One representative section for each of two grafts is shown. (a–c) Scale bar = 50 μm.

reperfusion as an activation sign of metabolic activity of intracellular functions. Pneumocytes type I function also as progenitor cells in response to lung injury. The development of MV could therefore also be considered as a prestage of an epithelial lung cell renewal. As such, MV seem to possess important functions in the early course of I/R injury. Intriguingly, MV also developed on the surface of the endothelium. In contrast, no MV were found in the right, non-transplanted lung, thus excluding a preparation artefact of the graft.

The thickening of the alveolar wall is a well-recognized histological hallmark of I/R injury. Accordingly, we found pneumocytes type II increasingly enlarged from 30 min towards 4 h of reperfusion. Also, we found MV to be densely located on the border between pneumocytes type I as a sign of greater activity of these cells. We assume that the electroneutrality homeostasis, which is conserved under normal conditions through paracellular tight junctions, is disturbed thereby promoting interstitial oedema and swelling of pneumocytes. The presence of interalveolar perforations that were detected after reperfusion might further support this hypothesis. Furthermore, we detected a widening of the perivascular space that reflects the development of oedema 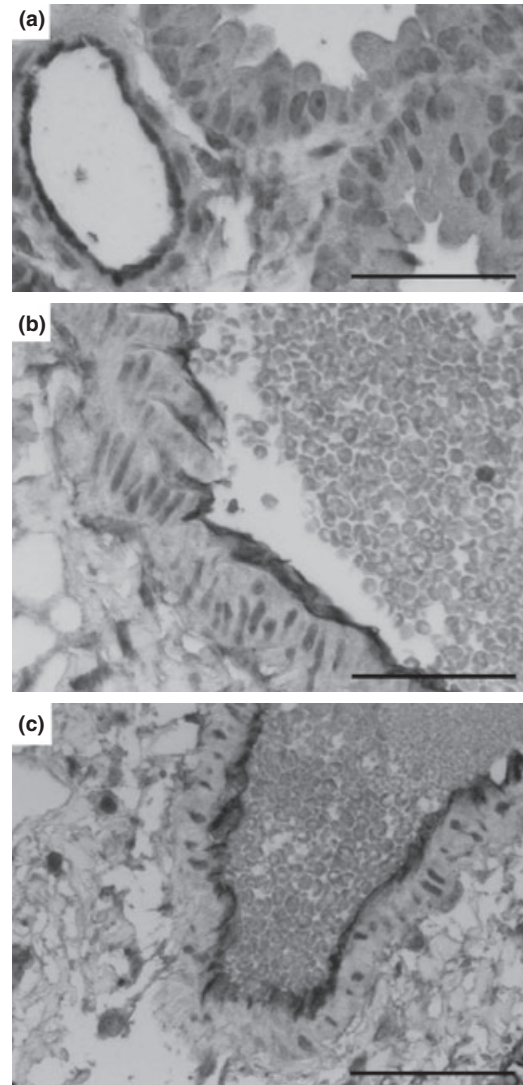in a different pulmonary compartment. The enlargement of the perivascular space could be attributed to a release of proinflammatory cytokines from transmigrating mononuclear cells.

Surfactant is crucial for a normal function of the endothelium-capillary compound. Once discontinued, the gas exchange is severely impaired. The exact mechanisms by which surfactant alterations in I/R injury occur are not completely understood. Most likely, oxidant species interact with surfactant components, in particular with surfactant apoproteins (Putman *et al.* 1997) and could therefore induce surfactant disruptions on the alveolar lining.

The occurrence of the disrupted surfactant layer provides evidence to an early damage to the blood gas barrier that impairs gas exchange already within minutes after reperfusion. This phenomenon is not observed in regular histology. Kohn pores that are invisible under normal conditions in non-injured lungs were detectable after reperfusion suggesting a lack in the surfactant layer. The alveolar lining of the right, non-transplanted lung showed an intact and continuous surface lining, suggesting that the I/R injury is likely to be the cause for the disruption of the surfactant layer. Surprisingly, surfactant was already lacking after the cold ischaemia time we applied, which emphasizes the deleterious effects of ischaemia injury alone. Attempts to renew the surfactant layer were undertaken and seem to be an important target for the reconditioning of ex vivo perfused organs (Inci *et al.* 2008; Muhlfeld *et al.* 2009).

The pathological changes described need to be critically viewed in regard to possible artefacts that may occur during the process of graft preparation. We immediately perfused the lungs with buffer followed by glutaraldehyde while the heart was still beating. Thus, a stable circulation could be maintained with equal perfusion of the solution. Yet, slight changes in the alveolar surface and changes between surfactant and the fixation medium are sometimes unavoidable when starting the fixation and dehydration process. This might contribute to misinterpreting pathological changes. Also, too much pressure during ventilation impacts the alveolar surface tension and may influence the results. However, the preserved surface of erythrocytes that are displayed in our specimens served as a reference of stable fixation.

Taken together, a thorough analysis of I/R injury in lung transplants using SEM enables to detect early pathomorphological changes. These observations add valuable data to conventional histology that were previously not reported. The knowledge about these changes provides the basis for a better interpretation when I/R injury is studied in the model of orthotopic mouse lung transplantation.

Acknowledgements

References

Bachofen H., Ammann A., Wangensteen D., Weibel E.R. (1982) Perfusion fixation of lungs for structure-function analysis: credits and limitations. *J. Appl. Physiol.* **53**, 528–533.

Bastacky J. & Goerke J. (1992) Pores of Kohn are filled in normal lungs: low-temperature scanning electron microscopy. *J. Appl. Physiol.* **73**, 88–95.

Dobbs L.G., Johnson M.D., Vanderbilt J., Allen L., Gonzalez R. (2010) The great big alveolar TI cell: evolving concepts and paradigms. *Cell Physiol. Biochem.* **25**, 55–62.

Eppinger M.J., Jones M.L., Deeb G.M., Bolling S.F., Ward P.A. (1995) Pattern of injury and the role of neutrophils in reperfusion injury of rat lung. *J. Surg. Res.* **58**, 713–718.

Eppinger M.J., Deeb G.M., Bolling S.F., Ward P.A. (1997) Mediators of ischemia-reperfusion injury of rat lung. *Am. J. Pathol.* **150**, 1773–1784.

Fehrenbach H., Schepelmann D., Albes J.M. *et al.* (1999) Pulmonary ischemia/reperfusion injury: a quantitative study of structure and function in isolated heart-lungs of the rat. *Anat. Rec.* **255**, 84–89.

Graf R., Schiesser M., Lussi A., Went P., Scheele G.A., Bimmler D. (2002) Coordinate regulation of secretory stress proteins (PSP/reg, PAP I, PAP II, and PAP III) in the rat exocrine pancreas during experimental acute pancreatitis. *J. Surg. Res.* **105**, 136–144.

Hasaniya N.W., Premaratne S., Zhang W.W. *et al.* (2009) Ischemia-reperfusion injury in the lung: quantitation using electron microscopy. *Vasc. Endovascular Surg.* **43**, 170–177.

Hsia C.C., Hyde D.M., Ochs M., Weibel E.R. (2010) An official research policy statement of the American Thoracic Society/ European Respiratory Society: standards for quantitative assessment of lung structure. *Am. J. Respir. Crit. Care Med.* **181**, 394–418.

Inci I., Ampollini L., Arni S. *et al.* (2008) Ex vivo reconditioning of marginal donor lungs injured by acid aspiration. *J. Heart Lung Transplant.* **27**, 1229–1236.

Jungraithmayr W.M., Korom S., Hillinger S., Weder W. (2009) A mouse model of orthotopic, single-lung transplantation. *J. Thorac. Cardiovasc. Surg.* **137**, 486–491.

Lee J.C. & Christie J.D. (2009) Primary graft dysfunction. *Proc. Am. Thorac. Soc.* **6**, 39–46.

Muhlfeld C., Schaefer I.M., Becker L. *et al.* (2009) Pre-ischaemic exogenous surfactant reduces pulmonary injury in rat ischaemia/reperfusion. *Eur. Respir. J.* **33**, 625–633.

Okazaki M., Krupnick A.S., Kornfeld C.G. *et al.* (2007) A mouse model of orthotopic vascularized aerated lung transplantation. *Am. J. Transplant.* **7**, 1672–1679.

Ovechkin A.V., Lominadze D., Sedoris K.C., Robinson T.W., Tyagi S.C., Roberts A.M. (2007) Lung ischemia-reperfusion injury: implications of oxidative stress and platelet-arteriolar wall interactions. *Arch. Physiol. Biochem.* **113**, 1–12.

Premaratne S., Razzuk A.M., Hasaniya N.W. *et al.* (2000) Scanning electron microscopic changes in the morphology of rabbit pulmonary tissue biopsied following ischemia and reperfusion: a window of opportunity? *J. Electron. Microsc. (Tokyo)* **49**, 675–679.

Putman E., van Golde L.M., Haagsman H.P. (1997) Toxic oxidant species and their impact on the pulmonary surfactant system. *Lung* **175**, 75–103.

Zanotti G., Casiraghi M., Abano J.B. *et al.* (2009) Novel critical role of Toll-like receptor 4 in lung ischemia-reperfusion injury and edema. *Am. J. Physiol. Lung Cell. Mol. Physiol.* **297**, L52–L63.